Damage Analysis for Mixed Mode Crack Initiation

Y. Wei, C.L. Chow[1], C.T. Liu[2]

Abstract: The paper presents a numerical simulation for mixed mode crack initiation based on the concepts of damage mechanics. A model with two scalar damage variables is introduced for characterization of damage in a material element. Then a tangent modulus tensor is derived for damage-coupled constitutive equations. A failure criterion is developed with the concept of damage accumulation not only to identify the location of damaged element where the crack initiation angle but also to determine the critical load for mixed mode fracture. The damage model developed is incorporated in a general-purpose finite element program ABAQUA through its UMAT subroutine. The finite element program is then used to perform numerical simulation for pre-cracked specimens under monotonic tensile loading. The thin plates are made of aluminum alloy and particulate composite embedded with a crack of inclined angle $\beta = 0^\circ$, 30°, 45° and 60° for mixed mode fracture analysis. The predicted crack initiation loads and the angles of crack initiation agree well with the test results.

1 Introduction

Most conventional approaches for mixed mode fracture prediction are based on the theory of fracture mechanics. The fracture parameters, such as the stress intensity factor K_C and the strain energy release rate G_C for brittle materials, the J-integral and COD for ductile materials, have been widely applied to conduct fracture analysis of engineering components containing a macro-crack. However, an important mechanism of failure in the materials is attributed to the presence of micro-cracks/voids. These micro-defects result in changes of mechanical property in the form of material degradation due to initiation, growth and coalescence of these micro-defects. Complete avoidance of such material damage is not realistic, especially for stress analysis at a crack tip. In addition, research results have cast doubts on the validity of the J-integral and COD as intrinsic material properties for ductile fracture, which by definition should be independent of geometry and loading history [Giovanola and Finnie (1984b,a); Liu and Zhuang (1985)].

The material damage has been successfully characterized with the theory of damage mechanics first introduced by Kachanov (1958) and later developed by many researchers [Lemaitre and Chaboche (1990); Krajcinovic and Lemaitre (1987)]. With the introduction of averaging macro-variables (damage variables), the deterioration of materials as a result of the nucleation and growth of distributed material micro-defects can be determined quantitatively. Chow and Wang developed an anisotropic model which has been successfully applied to analyze mixed mode crack initiation and propagation of aluminum alloy 2024-T3 [Chow and Wang (1988, 1989b,a)]. The model is based on a second-order damage tensor. Considerable computing time is however required for the FEM analysis on the transformation between local coordinate system and principal damage coordinate system. For the sake of computing efficiency, Chow and Wei have recently proposed an isotropic damage model with two scalars [Chow and Wei (1999)]. This paper is intended to present an investigation on the application of the proposed damage model to characterize ductile behavior of two materials, including damage-coupled constitutive equations, finite element formulation and ductile fracture of mixed mode crack.

2 Damage-Coupled Constitutive Equations

The gradual deterioration of the material under service due to nucleation and growth of micro-cracks or defects can be characterized with an internal state variable known as damage variable [Lemaitre and Chaboche (1990)]. Chow and Wei have recently developed a two-scalar damage model to evaluate damage accumulation under both monotonic and cyclic loading [Chow and Wei (1999)]. This section provides a brief description of the model required in the following sections for the development of finite element formulation.

Following the damage mechanics theory, the effective stress is defined as

$$\overline{\sigma} = \mathbf{M}(\mathbf{D}) : \sigma \tag{1}$$

where σ is the true stress tensor, $\mathbf{D}$ is the damage tensor and $\mathbf{M}(\mathbf{D})$ is the damage effect tensor which can be expressed as

$$\mathbf{M}(\mathbf{D}) = \frac{1}{1-D}\begin{bmatrix} 1 & \mu & \mu & 0 & 0 & 0 \\ \mu & 1 & \mu & 0 & 0 & 0 \\ \mu & \mu & 1 & 0 & 0 & 0 \\ 0 & 0 & 0 & 1-\mu & 0 & 0 \\ 0 & 0 & 0 & 0 & 1-\mu & 0 \\ 0 & 0 & 0 & 0 & 0 & 1-\mu \end{bmatrix} \tag{2}$$

D and μ are two scalar variables to characterize damage accumulation in materials. The thermodynamic conjugate forces

[1] Department of Mechanical Engineering, University of Michigan-Dearborn, Dearborn, MI 48128, USA

[2] Air Force Research Laboratory, Edwards AFB, CA 93524-7680

of the damage variables D and μ, known as the damage energy release rate, can be derived from the Helmholtz free energy ψ as

$$Y_D = -\rho\frac{\partial\psi}{\partial D} = -\frac{1}{1-D}\sigma^T : \mathbf{C}^{-1} : \sigma$$
$$Y_\mu = -\rho\frac{\partial\psi}{\partial \mu} = -\frac{1}{1-D}\sigma^T : \mathbf{Z} : \sigma \tag{3}$$

where $\mathbf{C}$ is the elastic tensor for damaged materials

$$\mathbf{C}^{-1} = \frac{1}{E}\times \begin{bmatrix} 1 & -\nu & -\nu & 0 & 0 & 0 \\ -\nu & 1 & -\nu & 0 & 0 & 0 \\ -\nu & -\nu & 1 & 0 & 0 & 0 \\ 0 & 0 & 0 & 2(1+\nu) & 0 & 0 \\ 0 & 0 & 0 & 0 & 2(1+\nu) & 0 \\ 0 & 0 & 0 & 0 & 0 & 2(1+\nu) \end{bmatrix}$$

The tensor $\mathbf{Z}$ can be expressed as

$$\mathbf{Z} = \frac{1}{E_0(1-D)}\times \begin{bmatrix} z_1 & z_2 & z_2 & 0 & 0 & 0 \\ z_2 & z_1 & z_2 & 0 & 0 & 0 \\ z_2 & z_2 & z_1 & 0 & 0 & 0 \\ 0 & 0 & 0 & 2(z_1-z_2) & 0 & 0 \\ 0 & 0 & 0 & 0 & 2(z_1-z_2) & 0 \\ 0 & 0 & 0 & 0 & 0 & 2(z_1-z_2) \end{bmatrix}$$
$$z_1 = 2\mu(1-\nu_0) - 2\nu_0$$
$$z_2 = (1+\mu)(1-\nu_0) - 2\mu\nu_0 \tag{4}$$

E and ν are respectively the effective Young's modulus and effective Poisson's ratio for damaged material. The relationships between E and ν and the damage variables D and μ are established as

$$E = \frac{E_0(1-D)^2}{1-4\nu_0\mu+2(1-\nu_0)\mu^2}$$
$$\nu = \frac{\nu_0 - 2(1-\nu_0)\mu - (1-3\nu_0)\mu^2}{1-4\nu_0\mu+2(1-\nu_0)\mu^2} \tag{5}$$

E_0 and ν_0 are the values of Young's modulus and Poisson's ratio for intact or undamaged material.

The elastic law of damaged material can be expressed in the effective stress-effective strain space as

$$\overline{\sigma} = \mathbf{C}_0 : \overline{\varepsilon}^e \tag{6}$$

where $\mathbf{C}_0$ is the initial elastic tensor for undamaged material. The yield surface is postulated with the concept of the effective stress as

$$F_p(\overline{\sigma}, R) = \sigma_p - [R_0 + R(p)] = 0 \tag{7}$$

where σ_p is the effective equivalent stress

$$\sigma_p = \left\{\frac{1}{2}\overline{\sigma}^T : \mathbf{H}_0 : \overline{\sigma}\right\}^{1/2} = \frac{1-\mu}{1-D}\sigma_{eq} \tag{8}$$

σ_{eq} is the Von-Mises equivalent stress, $\mathbf{H}_0$ is the plastic characteristic tensor for undamaged material, R_0 is the yield stress, p is the effective equivalent plastic strain, and R is the strain hardening threshold. The constitutive equations of plasticity for damaged materials are accordingly derived in the effective stress-effective strain space as

$$d\overline{\varepsilon}^p = \lambda_p\frac{\partial F_p}{\partial\overline{\sigma}} \tag{9}$$
$$dp = \lambda_p\frac{\partial F_p}{\partial(-R)} = \lambda_p \tag{10}$$

The plastic damage surface is formulated with the thermodynamic conjugate forces of the plastic damage variables as

$$F_d(Y_d, B) = Y_d - [B_0 + B(w)] = 0 \tag{11}$$

where Y_d is the equivalent damage energy release rate postulated as

$$Y_d = \left\{\frac{1}{2}\left(Y_D^2 + \gamma Y_\mu^2\right)\right\}^{1/2} \tag{12}$$

B_0 is the initial plastic damage threshold, B is the plastic damage hardening, w is the overall plastic-damage, and γ is the damage evolution coefficient. The plastic damage evolution equations are

$$dD = -\lambda_d\frac{\partial F_d}{\partial Y_D} = -\frac{\lambda_d Y_D}{2Y_d}$$
$$d\mu = -\lambda_d\frac{\partial F_d}{\partial Y_\mu} = -\frac{\lambda_d\gamma Y_\mu}{2Y_d}$$
$$dw = -\lambda_d\frac{\partial F_d}{\partial B} = \lambda_d \tag{13}$$

where λ_d is the Lagrange multiplier.

3 Finite Element Formulation

The proposed damage model is discretized and coded in the user subroutine UMAT of a finite element package known as ABAQUS (version 5.8). The implementation aims at providing a tool for numerical analysis based on the proposed damage model and validating the model by comparing its predictions with experimental measurements. The procedure is similar in principle to the conventional FEM analysis, except that the tangent modulus tensor is coupled with the damage variables. The formulation of the tangent modulus tensor is derived as follows.

The total elastic strain shown in Eq. 6 can be alternatively written as

$$d\overline{\sigma} = \mathbf{C}_0 : d\overline{\varepsilon}^e = \mathbf{C}_0 : d\overline{\varepsilon} - \mathbf{C}_0 : d\overline{\varepsilon}^p \tag{14}$$

Multiplying the above equation by $(\partial F_p/\partial\overline{\sigma})^T$ yields

$$\left(\frac{\partial F_p}{\partial\overline{\sigma}}\right)^T : d\overline{\sigma} = \left(\frac{\partial F_p}{\partial\overline{\sigma}}\right)^T : \mathbf{C}_0 : d\overline{\varepsilon} - \left(\frac{\partial F_p}{\partial\overline{\sigma}}\right)^T : \mathbf{C}_0 : d\overline{\varepsilon}^p \tag{15}$$

From the yield surface Eq. 7, we have

$$dF_p(\overline{\sigma}, R) = \left(\frac{\partial F_p}{\partial\overline{\sigma}}\right)^T : d\overline{\sigma} - \frac{dR}{dp}dp = 0 \tag{16}$$

$$\left(\frac{\partial F_p}{\partial\overline{\sigma}}\right)^T : d\overline{\sigma} = \frac{dR}{dp}dp \tag{17}$$

Substituting the Eqs. 9-10 and 16-17 into Eq. 15, we obtain the incremental plastic strain as

$$dp = \frac{\left(\frac{\partial F_p}{\partial\overline{\sigma}}\right)^T : \mathbf{C}_0 : d\overline{\varepsilon}}{\frac{dR}{dp} + \left(\frac{\partial F_p}{\partial\overline{\sigma}}\right)^T : \mathbf{C}_0 : \frac{\partial F_p}{\partial\overline{\sigma}}} \tag{18}$$

Thus the relationship between $d\overline{\sigma}$ and $d\overline{\varepsilon}$ is obtained with Eqs. 9-10, 14 and 18 as

$$d\overline{\sigma} = \mathbf{C}_0^{ep} : d\overline{\varepsilon} \tag{19}$$

where $\mathbf{C}_0^{ep}$ is the instantaneous tangent modulus tensor expressed as

$$\mathbf{C}_0^{ep} = \mathbf{C}_0 - \frac{\left(\mathbf{C}_0 : \frac{\partial F_p}{\partial\overline{\sigma}}\right) : \left(\mathbf{C}_0 : \frac{\partial F_p}{\partial\overline{\sigma}}\right)^T}{\frac{dR}{dp} + \left(\frac{\partial F_p}{\partial\overline{\sigma}}\right)^T : \mathbf{C}_0 : \left(\frac{\partial F_p}{\partial\overline{\sigma}}\right)} \tag{20}$$

From the definition of yield surface in Eq. 7,

$$\frac{\partial F_p}{\partial\overline{\sigma}} = \frac{1}{2\sigma_p}\mathbf{H}_0 : \overline{\sigma} = \frac{1}{2\sigma_p}\mathbf{H}_0 : \mathbf{M} : \sigma \tag{21}$$

Substituting it into Eq. 20, the tensor $\mathbf{C}_0^{ep}$ can be derived with Eq. 8 as

$$\mathbf{C}_0^{ep} = \mathbf{C}_0 - \frac{(\mathbf{C}_0 : \mathbf{H}_0 : \sigma) : (\mathbf{C}_0 : \mathbf{H}_0 : \sigma)^T}{4\sigma_{eq}^2\frac{dR}{dp} + (\mathbf{H}_0 : \sigma)^T : \mathbf{C}_0 : (\mathbf{H}_0 : \sigma)} \tag{22}$$

The above formulation of the instantaneous tangent modulus in Eq. 20 or 22 is expressed in terms of the incremental effective stress and strain in Eq. 19. However a finite element program such as ABAQUS is written in the true stress-true strain space. Therefore, it is necessary to transform Eq. 19 to the conventional stress-strain space as:

$$d\sigma = \mathbf{C}^{ep} : d\varepsilon \tag{23}$$

where $\mathbf{C}^{ep}$ is the effective instantaneous tangent modulus tensor in true stress-true strain space which can be derived and described in the following section.

From the definition of effective stress in Eq. 1,

$$d\overline{\sigma} = d\mathbf{M} : \sigma + \mathbf{M} : d\sigma \tag{24}$$

The relationships between the effective and true elastic strain and plastic strain are

$$\overline{\varepsilon}^e = \mathbf{M}^{T,-1} : \varepsilon^e \quad d\overline{\varepsilon}^p = \mathbf{M}^{T,-1} : d\varepsilon^p \tag{25}$$

Therefore, the effective strain is derived as

$$\begin{aligned} d\overline{\varepsilon} &= d\overline{\varepsilon}^e + d\overline{\varepsilon}^p = \mathbf{M}^{T,-1} : d\varepsilon + d\mathbf{M}^{T,-1} : \varepsilon^e \\ &= \mathbf{M}^{T,-1} : d\varepsilon - \mathbf{M}^{T,-1} : d\mathbf{M} : \mathbf{M}^{T,-1} : \varepsilon^e \end{aligned} \tag{26}$$

With the plastic damage evolution laws in Eq. 13, $d\mathbf{M}$ can be expressed as

$$d\mathbf{M} = \frac{\partial\mathbf{M}}{\partial D}dD + \frac{\partial\mathbf{M}}{\partial\mu}d\mu = -\left(\frac{\partial\mathbf{M}}{\partial D}\frac{\partial F_d}{\partial Y_D} + \frac{\partial\mathbf{M}}{\partial\mu}\frac{\partial F_d}{\partial Y_\mu}\right)dw \tag{27}$$

From the plastic damage surface expressed in Eq. 11

$$dF_d = \frac{\partial F_d}{\partial Y_D}dY_D + \frac{\partial F_d}{\partial Y_\mu}dY_\mu - \frac{dB}{dw}dw = 0 \tag{28}$$

Then, with the formulae

$$\begin{aligned} dY_D &= \left(\frac{\partial Y_D}{\partial\sigma}\right)^T : d\sigma + \frac{\partial Y_D}{\partial D}dD + \frac{\partial Y_D}{\partial\mu}d\mu \\ &= \left(\frac{\partial Y_D}{\partial\sigma}\right)^T : d\sigma - \left(\frac{\partial Y_D}{\partial D}\frac{\partial F_d}{\partial Y_D} + \frac{\partial Y_D}{\partial\mu}\frac{\partial F_d}{\partial Y_\mu}\right)dw \\ dY_\mu &= \left(\frac{\partial Y_\mu}{\partial\sigma}\right)^T : d\sigma + \frac{\partial Y_\mu}{\partial D}dD + \frac{\partial Y_\mu}{\partial\mu}d\mu \\ &= \left(\frac{\partial Y_\mu}{\partial\sigma}\right)^T : d\sigma - \left(\frac{\partial Y_\mu}{\partial D}\frac{\partial F_d}{\partial Y_D} + \frac{\partial Y_\mu}{\partial\mu}\frac{\partial F_d}{\partial Y_\mu}\right)dw \end{aligned} \tag{29}$$

Eq. 28 becomes

$$\begin{aligned} dw &= \mathbf{T} : d\sigma \\ \mathbf{T} &= \left[\frac{\partial F_d}{\partial Y_D}\left(\frac{\partial Y_D}{\partial\sigma}\right)^T + \frac{\partial F_d}{\partial Y_\mu}\left(\frac{\partial Y_\mu}{\partial\sigma}\right)^T\right] \Bigg/ \left[\frac{\partial Y_D}{\partial D}\left(\frac{\partial F_d}{\partial Y_D}\right)^2 + \right. \\ &\left. \frac{dB}{dw} + \left(\frac{\partial Y_D}{\partial\mu} + \frac{\partial Y_\mu}{\partial D}\right)\frac{\partial F_d}{\partial Y_D}\frac{\partial F_d}{\partial Y_\mu} + \frac{\partial Y_\mu}{\partial\mu}\left(\frac{\partial F_d}{\partial Y_\mu}\right)^2\right] \end{aligned} \tag{30}$$

Combining Eqs. 19, 23, 24, 26, 27 and 30, the effective instantaneous tangent modulus tensor is derived instead as

$$\mathbf{C}^{ep} = \mathbf{M}^{T,-1} : \mathbf{U}^{T,-1} : \mathbf{C}_0^{ep} : \mathbf{M}^{T,-1} \tag{31}$$

where

$$\begin{aligned} \mathbf{U} &= \mathbf{I} - \left(\mathbf{U}_0 + \mathbf{C}_0^{ep} : \mathbf{M}^{T,-1} : \mathbf{U}_0 : \mathbf{M}^{T,-1} : \mathbf{C}^{-1}\right) : \sigma : \mathbf{T} : \mathbf{M}^{T,-1} \\ \mathbf{U}_0 &= \frac{\partial\mathbf{M}}{\partial D}\frac{\partial F_d}{\partial Y_D} + \frac{\partial\mathbf{M}}{\partial\mu}\frac{\partial F_d}{\partial Y_\mu} \end{aligned} \tag{32}$$

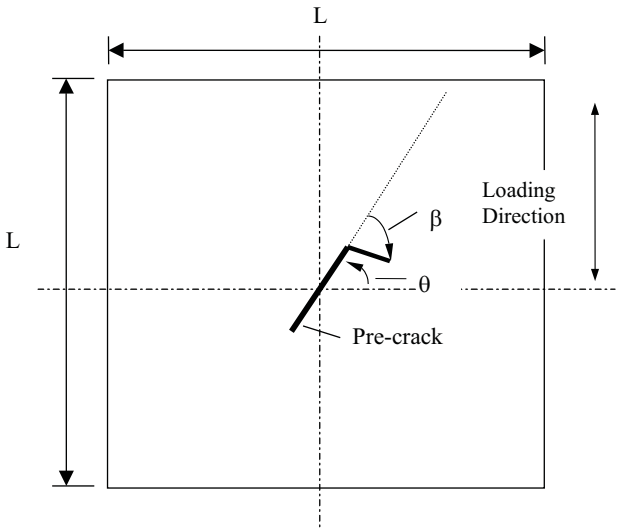

Figure 1 : Mixed mode specimen

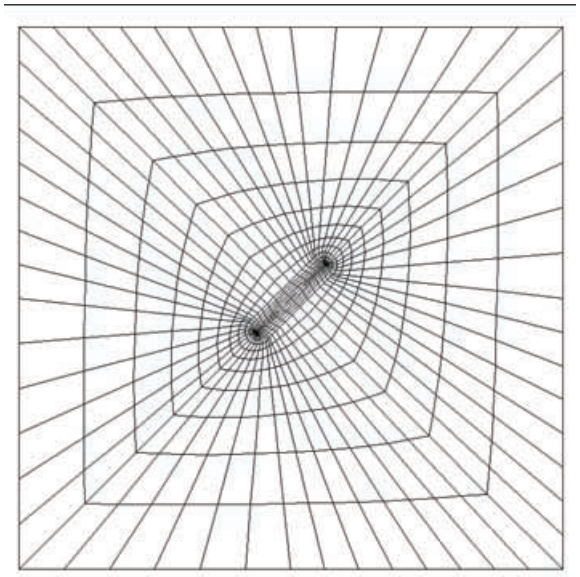

Figure 2 : Typical finite elements for mixed mode fracture analysis

In addition, the derivatives in Eq. 30 and 32 are derived as

$$\begin{aligned}
\frac{\partial Y_D}{\partial \sigma} &= -\frac{2}{1-D}\mathbf{C}^{-1}:\sigma \\
\frac{\partial Y_\mu}{\partial \sigma} &= -\frac{2}{1-D}\mathbf{Z}:\sigma \\
\frac{\partial Y_D}{\partial D} &= \frac{3}{1-D}Y_D \\
\frac{\partial Y_D}{\partial \mu} &= \frac{\partial Y_\mu}{\partial D} = \frac{2}{1-D}Y_\mu \\
\frac{\partial Y_\mu}{\partial \mu} &= -\sigma^T:\frac{\partial \mathbf{M}}{\partial \mu}:\mathbf{C}_0^{-1}:\frac{\partial \mathbf{M}}{\partial \mu}:\sigma
\end{aligned} \tag{33}$$

$$\begin{aligned}
\frac{\partial F_d}{\partial Y_D} &= \frac{Y_D}{2Y_d} \\
\frac{\partial F_d}{\partial Y_\mu} &= \frac{\gamma Y_\mu}{2Y_d}
\end{aligned} \tag{34}$$

$$\frac{\partial \mathbf{M}}{\partial \mu} = \frac{1}{1-D}\begin{bmatrix} 0 & 1 & 1 & 0 & 0 & 0 \\ 1 & 0 & 1 & 0 & 0 & 0 \\ 1 & 1 & 0 & 0 & 0 & 0 \\ 0 & 0 & 0 & -1 & 0 & 0 \\ 0 & 0 & 0 & 0 & -1 & 0 \\ 0 & 0 & 0 & 0 & 0 & -1 \end{bmatrix}$$

$$\frac{\partial \mathbf{M}}{\partial D} = \frac{1}{1-D}\mathbf{M} \tag{35}$$

$$\mathbf{M}^{-1} = (1-D)\times \begin{bmatrix} m_1 & m_2 & m_2 & 0 & 0 & 0 \\ m_2 & m_1 & m_2 & 0 & 0 & 0 \\ m_2 & m_2 & m_1 & 0 & 0 & 0 \\ 0 & 0 & 0 & m_1-m_2 & 0 & 0 \\ 0 & 0 & 0 & 0 & m_1-m_2 & 0 \\ 0 & 0 & 0 & 0 & 0 & m_1-m_2 \end{bmatrix}$$

$$\begin{aligned}
m_1 &= \frac{1+\mu}{1+\mu-2\mu^2} \\
m_2 &= -\frac{\mu}{1+\mu-2\mu^2}
\end{aligned} \tag{36}$$

Usually the matrix form of $\mathbf{C}^{ep}$ in Eq. 31 is a 6×6 asymmetric matrix for which most general purpose finite element programs may encounter computational convergency difficulties. Consequently, the symmetric form

$$\mathbf{C}^s = \frac{1}{2}\left(\mathbf{C}^{ep} + \mathbf{C}^{ep,T}\right) \tag{37}$$

is taken as a tangent modulus matrix when the finite element stiffness matrix is computed

$$\mathbf{K} = \int_v \mathbf{B}^T:\mathbf{C}^s:\mathbf{B} \tag{38}$$

where $\mathbf{B}$ is the transformation matrix.

4 Crack Initiation Angles for Al 2024-T3 Plates

A thin plate of aluminum alloy 2024-T3 containing an isolated crack was firstly investigated as shown in Fig.1. The

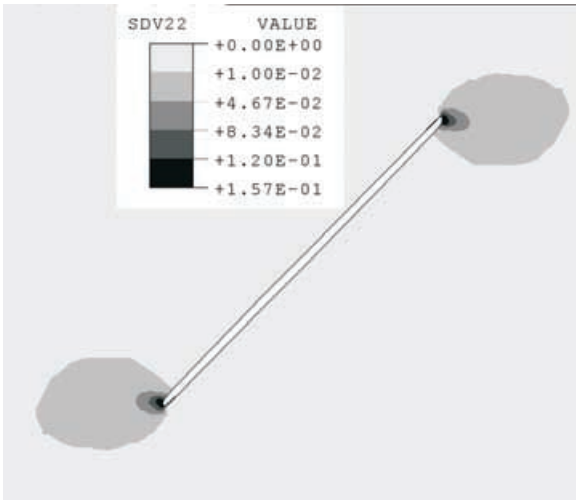

Figure 3 : Damage distribution contours in AL2024-T3 plate for $\theta = 45°$

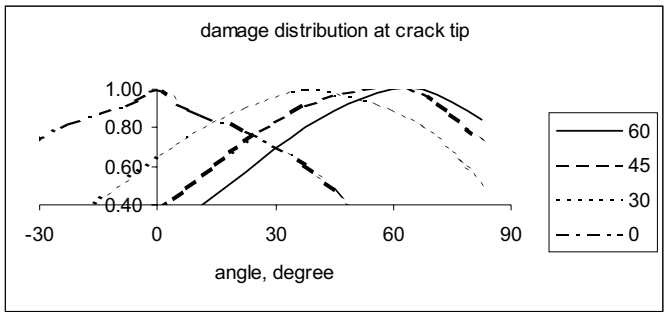

Figure 4 : Angular distributions of damage for mixed mode AL2024-T3 specimen

Table 1 : Crack Initiation Angle β_i for Al2024-T3 (characteristic crack length: 0.1 *mm*)

inclined angle	test	numerical proposed model	simulation anisotropic model
0	0	0	0
30	35.9	37.5	43
45	53.7	52.5	56
60	71.2	67.5	73

length dimension L is 86 *mm*, the thickness of the plate is 3.175 *mm* and the crack length is 15 *mm*. θ is the inclined angle of the isolated crack and β is the angle measured from the pre-crack direction. Different values of θ, namely 0°, 30°, 45° and 60°, are chosen for numerical simulation with ABAQUS (Version 5.8). Linear, reduced-integration solid elements are used for the FE analysis. A typical finite element discretization of the plate with a typical inclined crack of 45° is depicted in Fig.2. Radial elements were chosen around the crack tip for the convenience of determining angular distributions of overall damage at the crack tip. The mechanical properties of AL024-T3, which were determined and reported in reference [Chow and Wei (1999)], are summarized as:

$$E_0 = 74300\,MPa \quad \nu_0 = 0.34 \quad R_0 = 330\,MPa$$
$$\gamma = -0.4 \quad B_0 = 0.936\,MPa \quad w_c = 0.185$$

The overall damage distribution in the plate containing a typical inclined crack of 45° was calculated as shown in Fig.3. It can be observed from the figure that the damage accumulation is confined around the crack tip region. Crack initiation is postulated to occur at the location when the overall damage reaches its critical value. The direction of the crack extension β_i is determined from the detailed damage distribution at the crack tip. The angular distributions of the overall damage at the crack tip are calculated as shown in Fig.4 for different inclined cracks of 0°, 30°, 45° and 60°. The normalized damage at a constant radial distance from the crack tip was plotted against the angle of rotation β. The location of unit value of the normalized damage is used to determine the direction of crack extension, i.e. the initiation angle β_i.

Table 1 summarizes the predicted crack initiation angles for the mixed mode specimens. The measured and predicted results based on an anisotropic damage model reported by Chow and Wang are also included for comparison [Chow and Wang (1989b)]. It can be observed from the table that both of the numerical results agree well with the measured ones. An advantage of the proposed damage model is its ease of computation relative to the anisotropic damage model with a second-order tensor.

5 Fracture Analysis for Particulate Composite Plates

The boundary between the particles and the matrix in particulate composites constitutes the source of micro-defects, which will grow and coalescence until a macro-crack is formed under load. To ignore these micro-structural changes in the failure prediction by the conventional methods is not therefore considered realistic. The material deterioration due to damage accumulation should be taken into account for durability analysis with the theory of damage mechanics. The proposed damage model is accordingly applied to predict mixed mode fracture of a thin plate made of a particulate composite as shown in Fig.1. The dimensions of the plate are 4 *in* $\times$ 4 *in* $\times$ 0.2 *in*. The length of pre-crack is 1 *in*. and its inclined angle is represented by θ.

In order to determine mechanical properties and damage parameters for the particulate composite material, a modified dog-bone specimen is chosen for the measurement. The specimen is incrementally loaded at different strains until final rupture. Upon each incremental maximum strain, the specimen

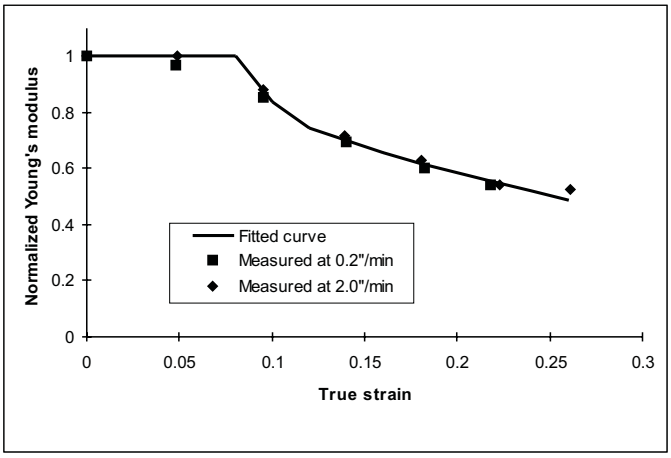

Figure 5 : Normalized Young's modulus vs applied strain for a particulate composite

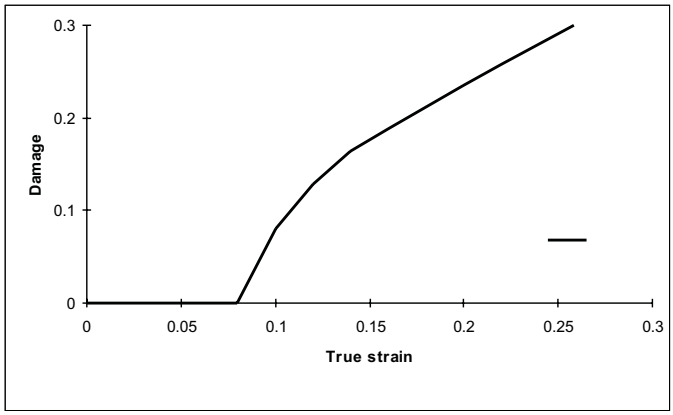

Figure 6 : Damage evolution curve for a particulate composite

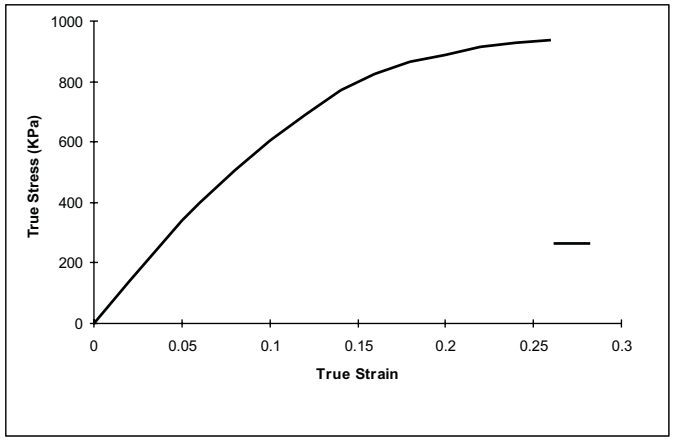

Figure 7 : True stress-true strain curve for a particulate composite

Table 2 : Crack Initiation Load for Particulate Composite (characteristic crack length: 1.4 *mm*)

Pre-crack angle (°)		0	30	60
Load	prediction	24.0	27.2	36.9
(*lb*)	test	23.4	27.0	36.2

Table 3 : Crack initiation Angle β_i (°) Particulate Composite (characteristic crack length: 1.4mm)

Pre-crack angle (°)		0	30	60
β_i	prediction	0	28	62
(°)	test	0	33	68

is unloaded to zero-stress, forming a hysteretic loop. The effective Young's modulus is determined after each unloading. The change of effective Young's modulus is taken as material degradation to evaluate the damage variable D as shown in Fig. 5 and 6. The true stress-true strain curve of the material is depicted in Fig.7. The value of D_c, which is considered an intrinsic material property, was determined to be 0.3. For the particulate composite, the value of Poisson's ratio is assumed to be constant during loading process. Accordingly, both the damage evolution coefficient γ and the damage variable μ are considered insignificant and thus assumed to be zero. Therefore, the damage model is simplified to the conventional isotropic damage model with one scalar damage variable.

The FE analysis is similar to the case example of AL2024-T3. The loading is applied through the displacement boundary condition. The element is postulated to be fully damaged and therefore failed when the plastic damage D at its integration point reaches a critical value Dc. The load applied at Dc is determined as crack initiation load and the position of damaged integration point is used to define the direction of crack extension, i.e. the crack initiation angle. Three different inclined crack angles, $\theta = 0^\circ$, $30^\circ$and 60°, are chosen for the analysis. The numerical results on the crack initiation angle and the fracture load are summarized in Table 2 and 3, demonstrating a satisfactory agreement with the experimental measurements.

6 Conclusions

Damage-coupled finite element formulation has been derived for the proposed damage model. The model has been implemented in ABAQUS (version 5.8) through its UMAT subroutine for failure analysis of mixed mode fracture. A failure criterion is developed to determine the crack initiation at the location where the overall damage accumulation reaches a critical value of the material. Therefore, the crack initiation angle and fracture load can be determined from the FEM results. Two engineering materials, AL2024-T3 and a particulate composite, are chosen for the investigation. A mixed mode fracture analy-

sis was carried out and the predicted results are compared well with the test data.

References

Chow, C. L.; Wang, J. (1988): Ductile fracture characterization with an anisotropic continuum damage theory. *Engineering Fracture Mrchanics*, vol. 30, pp. 547–563.

Chow, C. L.; Wang, J. (1989): Crack propagation in mixed-mode ductile fracture with continuum damage mechanics. *Proc Instn Mech Engrs*, vol. 203, pp. 189–199.

Chow, C. L.; Wang, J. (1989): On crack initiation angle of mixed mode ductile fracture with continuum damage mechanics. *Engineering Fracture Mrchanics*, vol. 32, pp. 601–612.

Chow, C. L.; Wei, Y. (1999): Constitutive modeling of material damage for fatigue failure prediction. *Int. J. Damage Mechanics*, vol. 8, pp. 355–375.

Giovanola, J. H.; Finnie, I. (1984): The crack-opening displacement (cod) as a fracture parameter and a comparative assessment of the cod and j-integral concepts. *SM Archives*, vol. 9, pp. 227–257.

Giovanola, J. H.; Finnie, I. (1984): A review of the use of the j-integral as a fracture parameter. *SM Archives*, vol. 9, pp. 197–225.

Kachanov, L. M. (1958): On creep rupture time. *Izv. Acad. Nauk SSSR Otd, Techn. Nauk*, vol. 8, pp. 26–31.

Krajcinovic, D.; Lemaitre, J. (1987): *Continuum damage mechanics theory and applications*. International Center for Mechanical Sciences Courses and Lectures, No. 295, Springer, Berlin.

Lemaitre, J.; Chaboche, J. L. (1990): *Mechanics of Solid Materials*. Cambridge University Press.

Liu, H. .; Zhuang, T. (1985): A dual parameter elastic-plastic fracture criterion. *International Journal of Fracture*, vol. 27, pp. R87–91.